IV International Conference and School "Advanced High Entropy Materials"
September 26-30, 2022

№62

OBTAINING OF SPHERICAL TITANIUM POWDER FOR USE IN ADDITIVE TECHNOLOGIES

ncherezov@ism.ac.ru

Cherezov N. P.[1], Fadeev A.A.[2]

[1]Merzhanov Institute of Structural Macrokinetics and Problems of Materials Science, Russian Academy of Sciences, Chernogolovka, Russia; [2]Baykov Institute of Metallurgy and Materials Science of the Russian Academy of Sciences, Moscow, Russia.

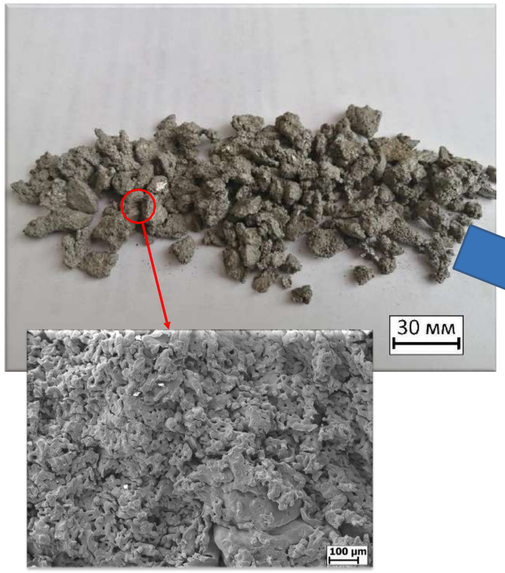

Initial material titanium sponge

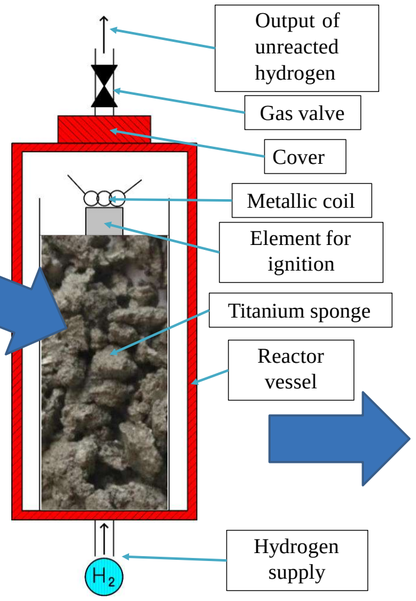

The process of SHS-hydrogenation of titanium sponge

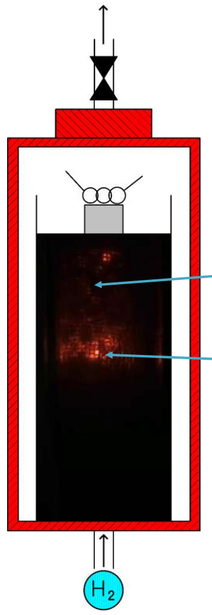

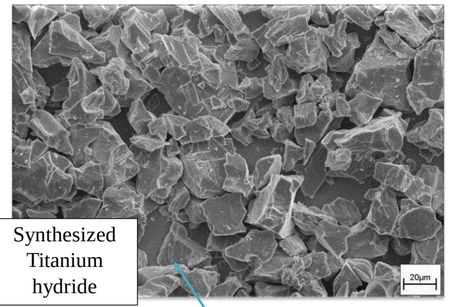

Mechanical grinding of hydrogenated titanium sponge

TiH_2

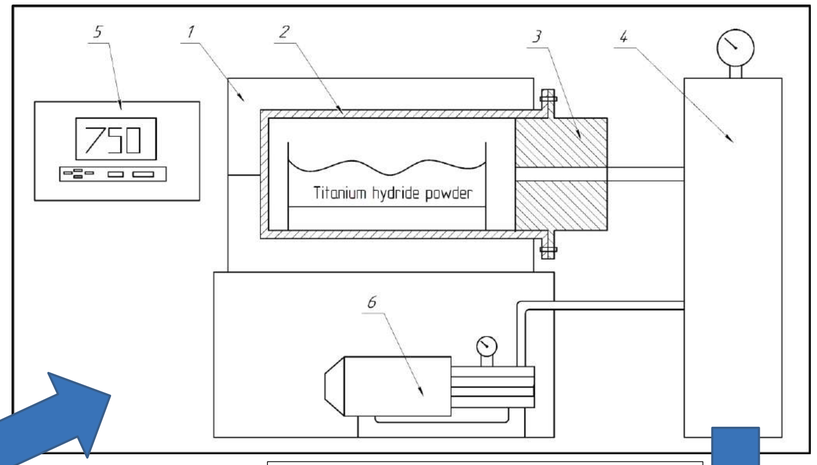

Hydrogen removal (dehydrogenation) of crushed titanium hydride

The main components of the dehydrogenation equipment:
1. Muffle electric furnace. 2. Dehydrator casing.
3. Dehydrator cover. 4. Vacuum receiver.
5. Furnace control panel. 6. Vacuum pump.

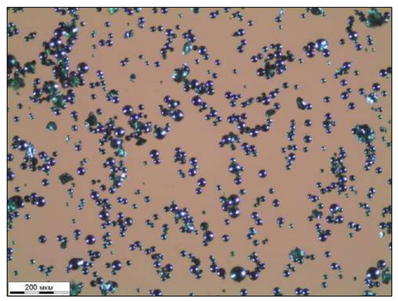

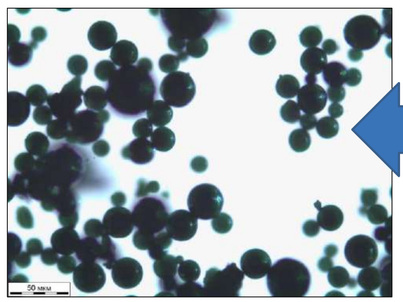

Finished product spherical titanium powder

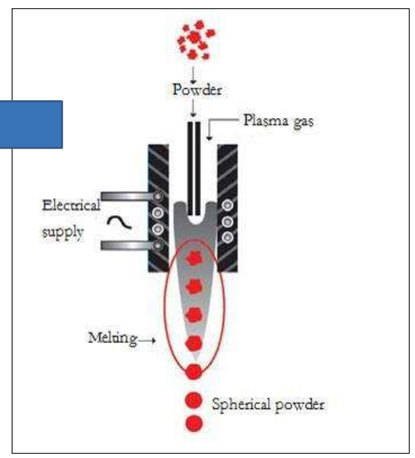

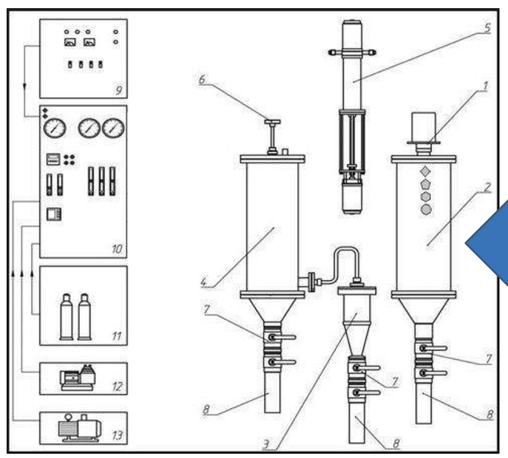

Patent No. 2756327, 2021

The process of spheroidization

The main components of the installation for spheroidization:
1. Electric arc generator of thermal plasma (plasmatron).
2.Plasma powder processing chamber. 3. Cyclone (optional). 4. Exhaust gas filtration apparatus. 5. Powder dispenser. 6. Filter cleaning system. 7. Powder unloading crane. 8. Product collection. 9. The power source of the plasma torch. 10. Sensor stand. 11. Gas supply system. 12. Water supply system. 13. Vacuum pump.

Plasma torch power, kW	26,4
Plasma-forming gas	Ar
Plasma flow enthalpy, kWh/m³	4,7
Powder consumption, kg/h	1

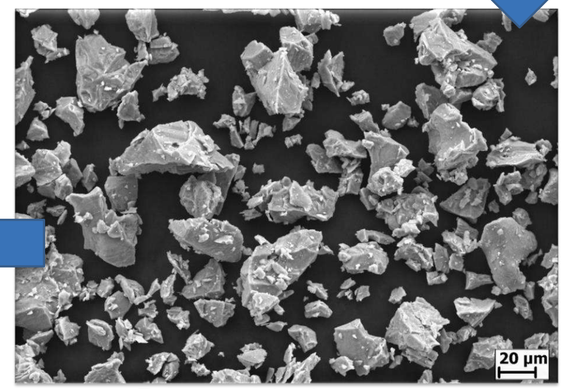

Dehydrated titanium powder

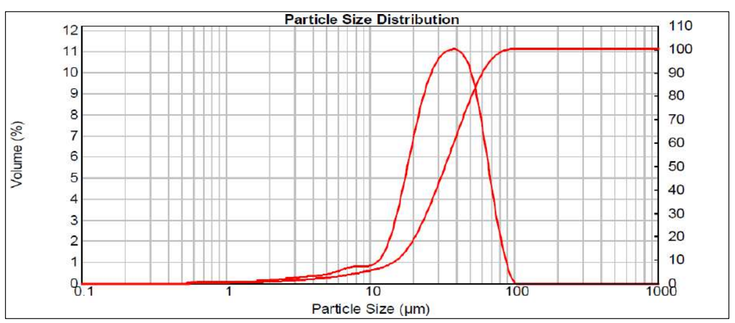

Characteristics of the dispersed composition (microns):
D_{10}= 15.5; D_{50}= 33.5; D_{90}= 60.7; D_{min}= 0,6; D_{max}= 97.

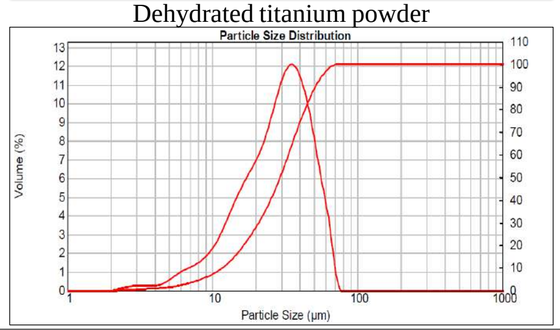

Characteristics of the dispersed composition (microns):
D_{10}= 11.7; D_{50}= 29.3; D_{90}= 51.1; D_{min}= 2,2; D_{max}= 72.

Shaysultanov@bsu.edu.ru

STRUCTURE AND MECHANICAL PROPERTIES OF A MEDIUM-ENTROPY TRIP ALLOY PRODUCED BY SELECTIVE LASER MELTING

Shaysultanov D. G., Povolyaeva E. A., Stepanov N. D. and Zherebtsov S. V.

Laboratory of Bulk Nanostructured Materials, Belgorod State University, 85 Pobeda Str., 308015, Belgorod, Russian Federation

Abstract

Recently, multicomponent alloys high-entropy and medium-entropy (HEAs and SESs)) with close to equiatomic element abundances have attracted considerable attention from materials scientists. This interest is due to the unusual properties demonstrate by the MEAs. In particular, some MEAs have a TRIP effect, which provides significant work hardening and, as a result, very high values of tensile strength and ductility are achieved. Compared to traditional manufacturing methods, selective laser melting (SLM) makes it possible to obtain treat difficult parts directly from powder, with control over all production parameters. The formation of a fine-grained microstructure and a uniform chemical composition by the section of the part is provided, due to the high crystallization rate during SLM. It is contributing to the achievement of a high level of mechanical properties. Meanwhile, there are no systematic data on the effect of SLM on the structure and mechanical properties of carbon-containing MEAs with the TRIP effect.

Material: $Fe_{65}(CoNi)_{25}Cr_{9.5}C_{0.5}$ medium-entropy alloy

I. Microstructure and mechanical properties of as-cast alloy

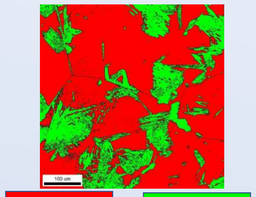

FCC - 65% BCC - 35%

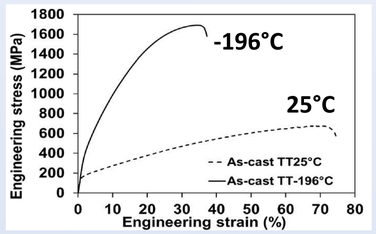

25°C EBSD phase maps of alloy after tensile test -196°C

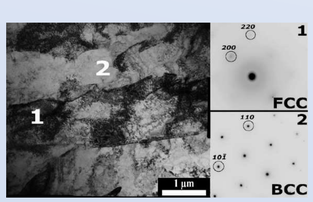

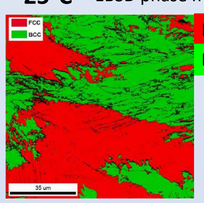

FCC- 54% BCC - 46%

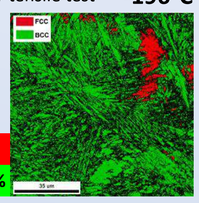

FCC- 3% BCC - 97%

Phase maps TEM image and stress-strain curves of as-cast alloy

II. Initial condition of powder

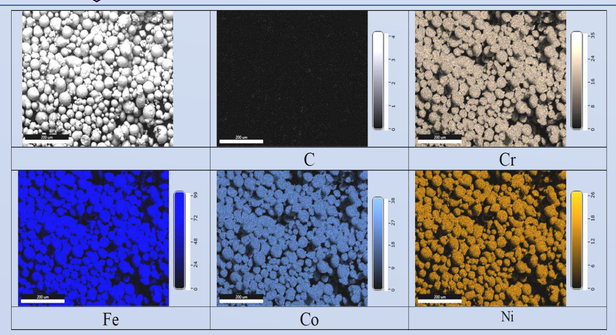

Elemental distribution maps

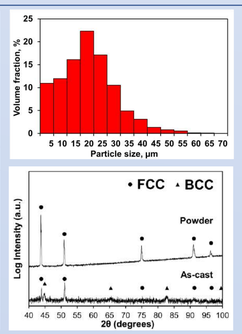

XRD patterns

III. Selection regime

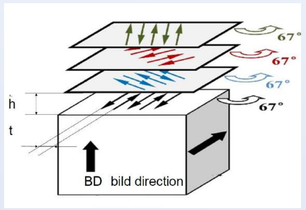

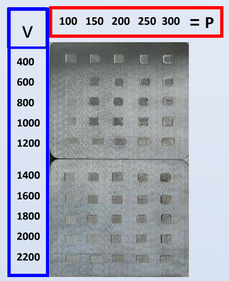

VED = P/V*t*h - volume energy density (VED), (J/mm³)

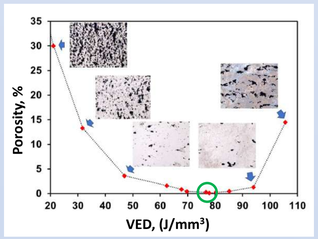

Dependence of the volume fraction of pores on volume energy density.

IV. Microstructure and mechanical properties of alloy after SLM

V=1600 mm/c, P= 200W

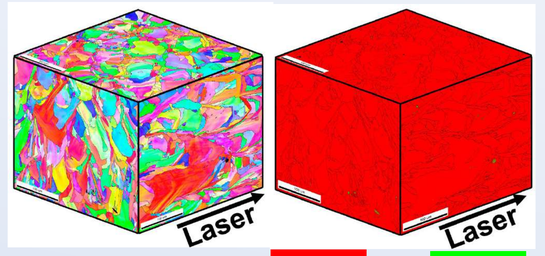

FCC - 99% BCC - 1%

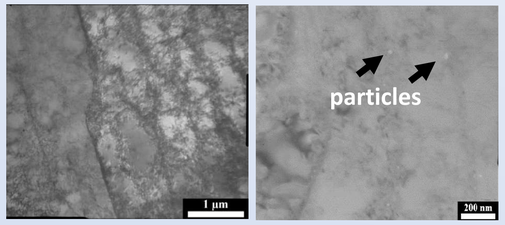

TEM images of alloy after SLM.

Mechanical properties of alloy

Condition	YS, MPa	UTS, MPa	TE, %
As-cast, 25°C	155	682	65
SLM, 25°C	572	660	36
As-cast, -196°C	375	1692	27
SLM, -196°C	700	1796	25

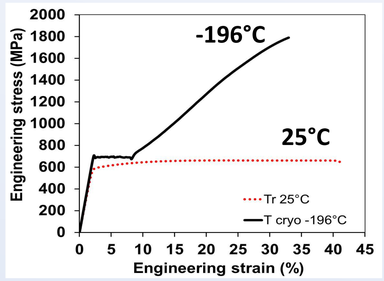

Stress-strain curves of alloy after SLM

EBSD phase maps of alloy after tensile test

25°C -196°C

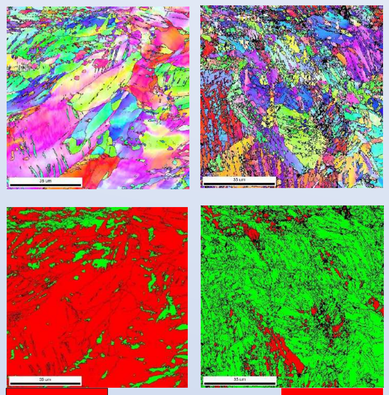

FCC – 86% BCC– 14% FCC- 8% BCC - 92%

Conclusion

During the work, the $Fe_{65}(CoNi)_{25}Cr_{9.5}C_{0.5}$ alloy was successfully fabricated by selective laser sintering. The developed SLM regime made it possible to obtain a product from an alloy with a minimum content of pores and an elongated microstructure with increased of dislocations density. It successfully contributed to the increase in ultimate strength and a three-fold increase in yield strength while maintaining optimal ductility compared to an alloy made in the traditional way at both room and cryogenic temperatures.

Financial support from the Russian Science Foundation (Grant No. 20-79-10093) is gratefully acknowledged. This work was carried out using equipment of the Joint Research Center of Belgorod State National Research University «Technology and Materials».

IV International Conference and School "Advanced High Entropy Materials"
September 26-30, 2022

№65

shvt1@tut.by

TECHNICAL CERAMICS (TC): PROBLEMS, PRINCIPLES AND MECHANISMS OF SCIENTIFIC-PRACTICAL DEVELOPMENT AND IMPLEMENTATION IN PRODUCTION

Shmuradko N.A., Panteleenko E.F., Panteleenko F.I., Bendik T.I., Shmuradko V.T., Vinogradov V.V.

1. Wear-resistant support rollers

2. Tribotechnical sealing elements

3. Rimmers for underground tunnelling

a)

b)

c)

4. Funnels for dosing metal melts

5. Ceramic flame retardant crucibles for dentistry

6. Thermal heat shields

7. Double layer dispenser cup (SD)

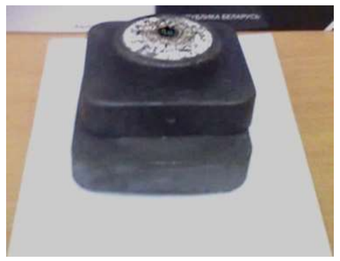

8. Double-layer SD of gate-type

9. Electrical insulator for electron beam welding

10. Heat-resistant electrical insulators for BelAZ

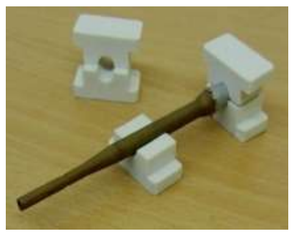

11. Electrical insulators for automatic bimetal welding

12. Vacuum-tight high-temperature electrical insulators for vacuum and other electric furnaces

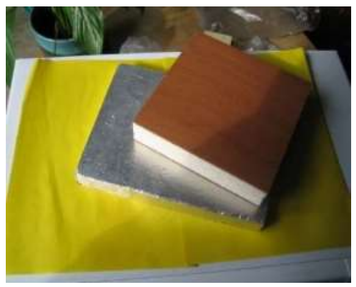

13. Refractory thermal insulation products vermiculite thermosetting (VT)

a)

b)

14. Emerald (a) and AQUAEHA (b) for the energy treatment and structuring of water and aqueous solutions

a)

b)

15. Porous capillary-permeable diaphragms (CPD) for electrochemical reactors (ECR) without and with functional thin-film (ion-plasma, magnetron) coatings for Izumrud and AQUAEHA installations

a)

b)

16. Billet (pressed) a) for the manufacture of high-energy fuel electrodes - monocrystals (thermal emitters) b) for plasma rocket engines (PRE)

IV International Conference and School "Advanced High Entropy Materials" September 26-30, 2022 №66

E-mail: pumnov@imet.ac.ru

Umnov P.P., Chueva T.R., Molokanov V.V., Palii N.A., Krutilin A.V., Bahteeva N.D.

PERSPECTIVES APPLICATIONS PRODUCTS FROM AMORPHOUS MICROWIRES FOR MEDICINE

A.A. Baikov Institute of Metallurgy and Materials Science, Moscow, Russia

The original technologies for obtaining:

✓ **amorphous microwires Ø 50-150 μm**

-various compositions (Fe-Co-Ni)-(Si,B),
-no need machining,
-low friction coefficient

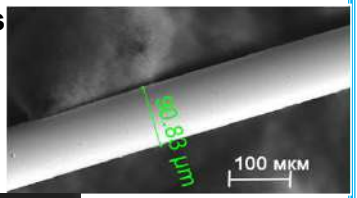

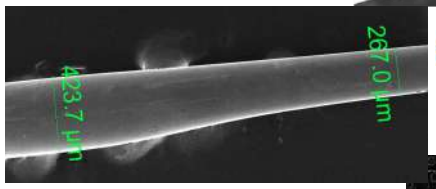

✓ **variable cross section microwires**

✓ **microspirals Ø 0,2–1 mm**

-cold plastic deformation without heat treatment,
-constant and variable rigidity

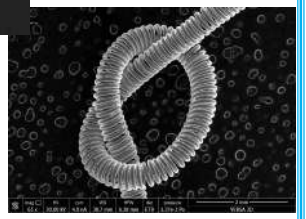

➢**High strength** ➢**Super-elasticity**

- exceeds of high-strength stainless steels and nitinol
- elastic tension to 3% of original length
- elastic twisting to 1 rev/cm without changing geometry of wire
- can be tightened into a knot without breaking)

➢**Excellent soft magnetic properties**

➢**Radiopacity** ➢**Biocompatibility**

➢**High corrosion resistance**

Mechanical properties	Physical properties	Magnetic properties
σ_B = 2500 ÷ 4000 MPa	γ = 7300 ÷ 7700 kg/m^3	B = 0,6 ÷ 1,0 T
$\sigma_\varepsilon \sim 0{,}9\sigma_B$	T_m = 950 ÷ 1100 ºC	H_C = 0,02 ÷ 0,50 Oe
ε = 2,5 ÷ 4%	T_C = 200 ÷ 520 ºC	μ = 10000 ÷ 200000
G = 120 ÷ 170 GPa	T_{cryst} = 480 ÷ 550 ºC	$\lambda_S > 0; < 0; \approx 0$
HV = 800 ÷ 1000	Δ T_{use} = -50 ÷ 150 ºC	
	ρ= 120 ÷ 140 μΩ·cm	

Applications

Stents

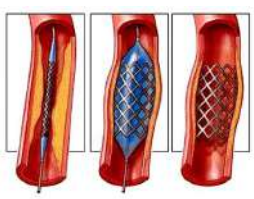

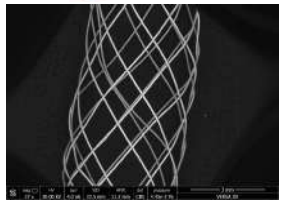

Examples of amorphous wire stent

Guides

for endovascular surgery

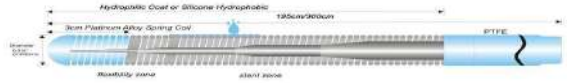

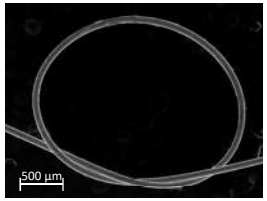

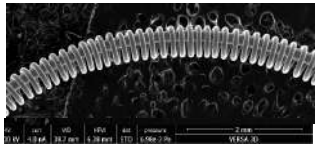

level or conical, Ø < 0,014"

Magnetic radiopaque markers

- for surgical tampons and napkins
- for labeling tubes

Magneto-vibrational influence

application napkins, cosmetic masks

Embols

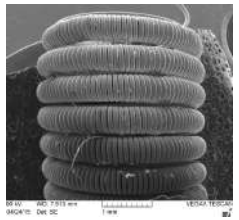

Examples of amorphous microspirals embolus

Thrombectomy device and cava filters

Pacemaker electrodes

Microcatheters

reinforcement

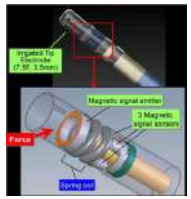

controlled

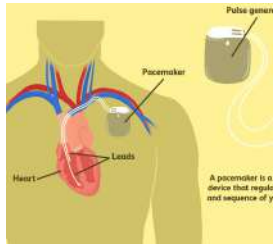

Medical microrobots

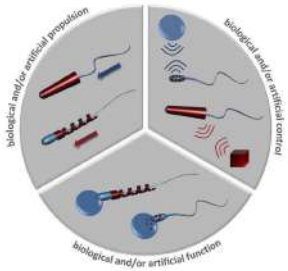

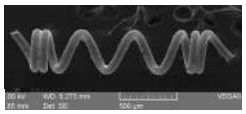

amorphous microwire microswimmers

targeted drug delivery

Amorphous microwires are perspective materials for medical applications due to the unique combination of physical, mechanical, tribological, corrosion properties, radiopacity, and biocompatibility

The work was carried out according to the state order №075-00715-22-00

' International Conference and School "Advanced High Entropy Materials"
September 26-30, 2022

№67

*yuzbekova@bsu.edu.ru

INFLUENCE TEMPERATURES OF TEMPERING ON MECHANICAL PROPERTIES OF STEEL 60Si2CrVNb

Yuzbekova D. Y.[1,2*], Dudko V. A.[1,2], Vetrova S. M.[1], Gaidar S. M.[1], Kaibyshev R. O.[1]

[1]Russian State Agrarian University-Moscow Timiryazev Agricultural Academy, Moscow, Russia

[2]Belgorod State National Research University, Belgorod, Russia

Chemical Compositions, mass%									
C	Si	Mn	Cr	V	Nb	Al	N	S	P
0,53	1,6	0,9	0,76	0,14	0,05	0,015	0,011	0,011	0,008

Mechanical properties of the steel

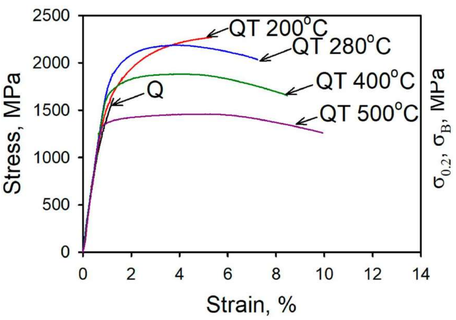

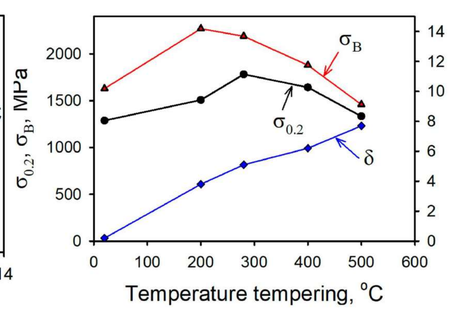

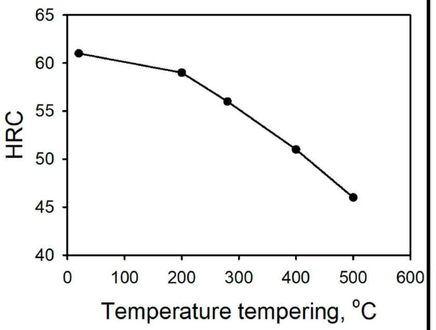

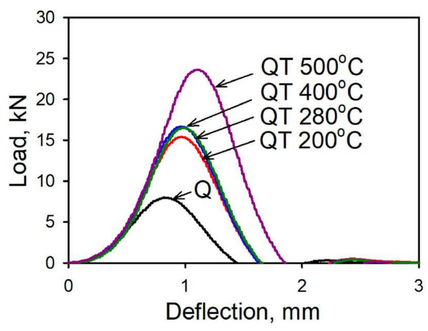

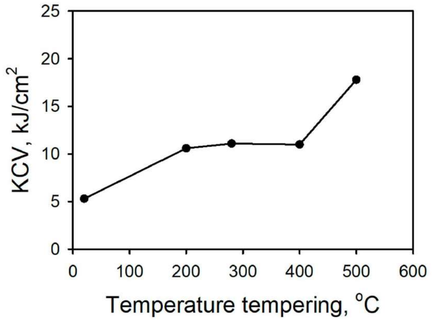

Mechanical properties of the steel after quenching from 900°C into water and tempering at different temperatures

Tempering temperature, °C	$\sigma_{0.2}$, MPa	σ_B, MPa	δ, %	δ_{true}, %	HRC	KCV, J/cm^2
20	1289	1630	0.2	0.5	61	5.3
200	1509	2270	3.8	4.2	59	11
280	1783	2190	5.1	6.2	56	11
400	1643	1880	6.2	7.6	51	11
500	1334	1460	7.7	9.3	46	18

Microstructure of the steel after quenching and tempering at 280°C

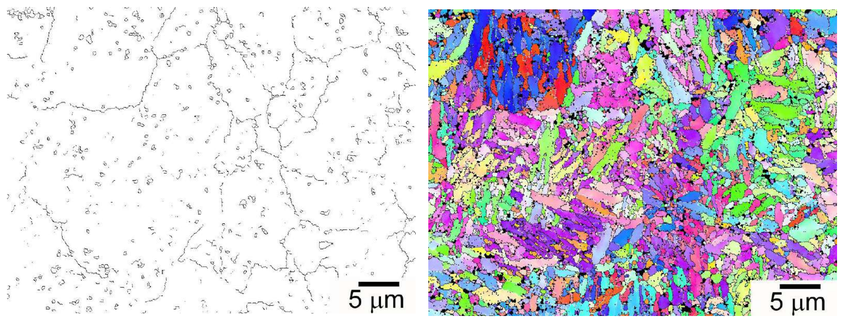

PAG size ~ 11 μm
Distance between HAB ~ 1.1 μm

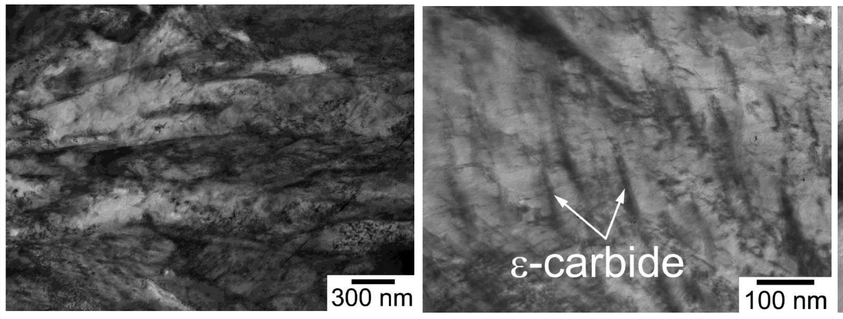

Lath size ~ 285 nm
Dislocation density ~ 1×10^{15} m^{-2}

ε-carbide size (width / length) ~ 14 / 89 nm

Carbonitrides size ~ 10 nm

Summary

1. High strength is retained in the steel after tempering at temperatures of 200 and 400°C;
2. Optimal combination between yield strength of 1783 MPa, ultimate tensile strength of 2190 MPa and elongation to failure of 6.2% are obtained after tempering at temperature of 280°C;
3. The microstructure after quenching and tempering at temperature of 280°C consists of lath martensite with laths size of 285 nm and dislocation density within laths 1 × 10^{15} m^{-2}. Tempering at temperature of 280°C results in precipitation of strip-like ε-carbide.
4. Noticeable decrease in strength occurs after tempering at 500°C, when yield stress decreased to 1334 MPa and ultimate tensile strength decreased to 1460 MPa.

The financial support received from the Ministry of Science and Higher Education of the Russian Federation, project No. 075-15-2021-572, is gratefully acknowledged. The work was carried out using equipment of the Joint Research Center of Belgorod State National Research University «Technology and Materials».

zakharov@ism.ac.ru

Zakharov K.V., Andreev D.E., Yukhvid V.I., Sanin V.N.

INFLUENCE OF THE Co CONTENT ON THE THE COMPOSITION AND STRUCTURE FORMATION OF CAST ALLOYS Co—Cr—Nb—W—Mo—Al—C IN THE PROCESS OF CENTRIFUGAL SHS-METALLURGY

Co-based cast alloys have high strength at high temperature and are used in gas turbine engines. In this paper, the task is to investigate the possibility of obtaining alloys with different ratios of Co and alloying additives (Cr—Nb—W—Mo—Al—C) by centrifugal SHS metallurgy and controlling their composition and structure.

To obtain cast alloys, mixtures of (Cr_2O_3/Nb_2O_5/WO_3/MoO_3/Al/C) + x (Co_3O_4/Al) with x from 0 to 100 wt% were used. Under atmospheric conditions, the combustion of mixtures is accompanied by an intense dispersion of combustion products. The effect of overload suppresses the spread and allows you to get cast alloys with different ratios of cobalt and alloying elements (Cr, Nb, Mo, W, C and Al). With an increase in the content of Co_3O_4 from 0 to 100% wt. in the mixture, the combustion rate increases ~5 times, and the yield of target elements into the ingot approaches the calculated values, the Co content in the alloy increases monotonically, the content of Nb, Mo, W, C decreases and the Al content passes through a maximum.

In cast alloys, a Co-based matrix is formed in which the NbC is distributed. The change in the phase composition is accompanied by a change in the microstructure from globular to dendritic.

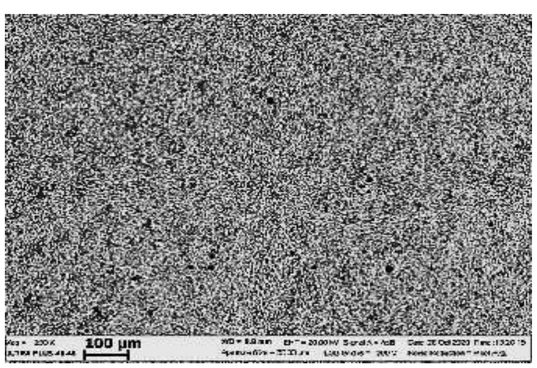

Co = 0 wt %

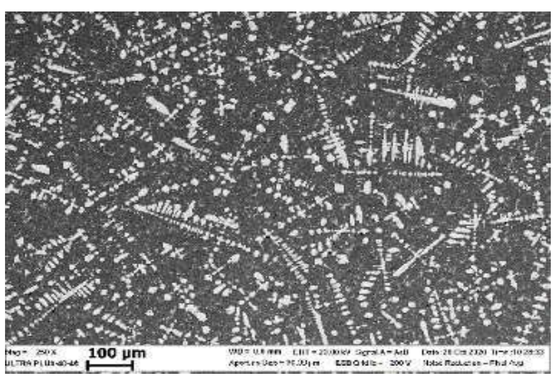

Co = 50 wt %

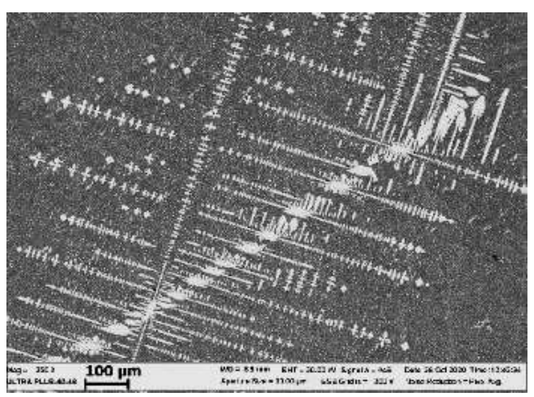

Co = 70 wt %

Effect of cobalt content on alloy microstructure

IV International Conference and School "Advanced High Entropy Materials"
September 26-30, 2022

№73

sokolovskiy@bsu.edu.ru

The effect of microstructure parameters on strength and ductility of β-solidified γ-TiAl based alloy

Sokolovsky V.S., Salishchev G.A.

The effect of microstructure parameters on mechanical properties of the β-solidified Ti-44Al-2V-1Nb-1Cr-0.1Gd alloy under tension was studied. Ingot in the as-cast condition was subjected to thermomechanical and subsequent two-step heat treatment to obtained conditions with different parameters. The interlamellar spacing (λ) was ranged from 70 to 1000 nm, remaining the same colony size of 70 μm. The tensile stress-strain curves and the resulting mechanical properties were obtained. The alloy with λ~150 nm demonstrated the maximum values of ductility under tensile – 1.5 %. Both increasing and decreasing of interlamellar spacing resulted in significant drop in the ductility. The alloy with lower colony size of 15 μm and λ~80 nm achieved much more strength and ductility, was 750 MPa and 4.5 %, respectively.

Interlamellar spacing
λ=70, 150, 1000 nm

Colonies size
D=70 μm=const

Volume fraction of colonies
V=85%=const

λ=70 нм

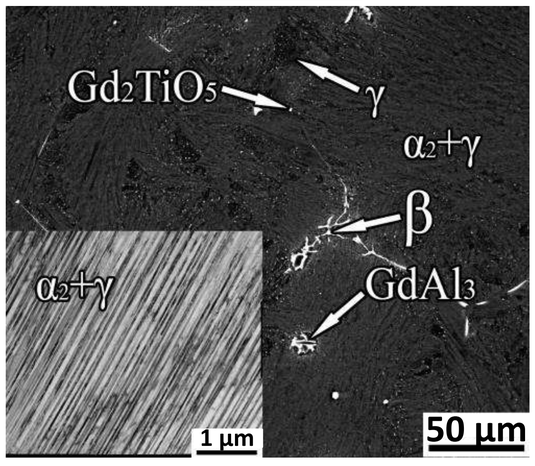

λ=150 nm

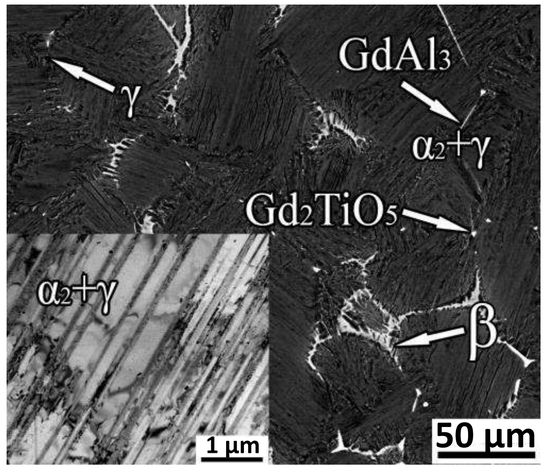

λ=1000 nm

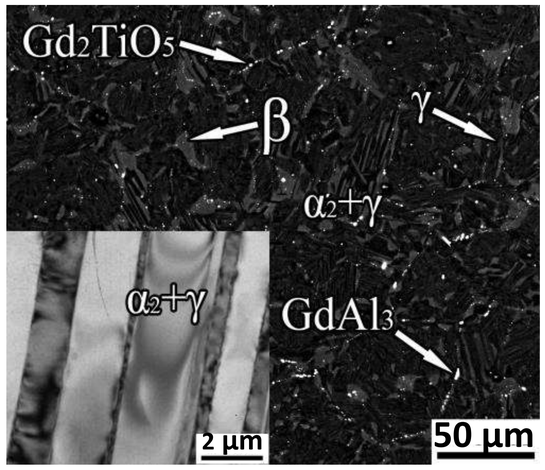

Interlamellar spacing λ=80 nm

Colonies size D=15 μm

Volume fraction of colonies V=45%

λ=80 nm

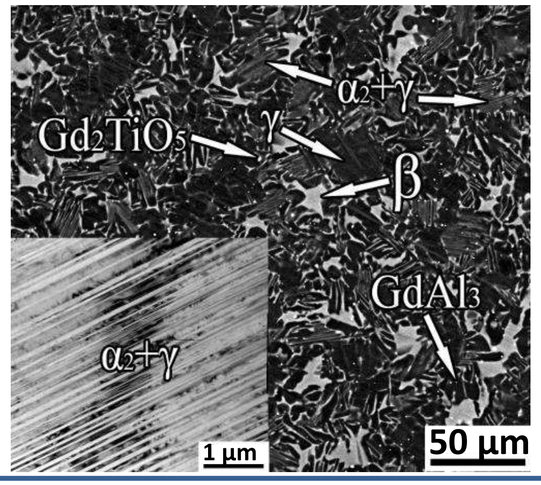

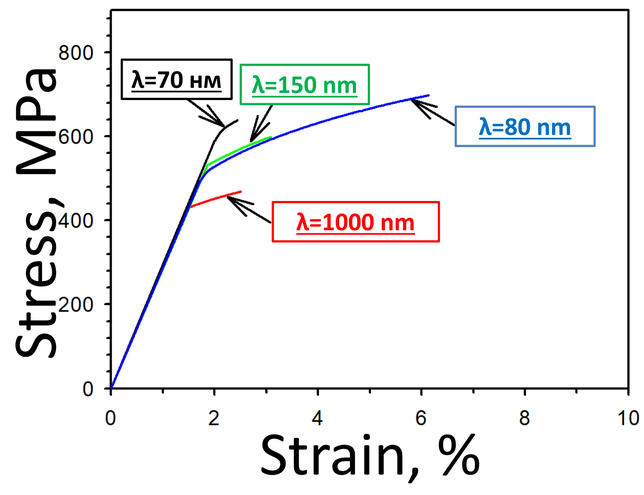

Conclusion The Ti-44Al-2V-1Nb-1Cr-0.1Gd alloy with the same volume fraction and size of colonies, a decrease in λ leads to an increase in σ_B and, initially, to an increase in δ (max at λ=150 nm), and then its decrease. A decrease in the volume fraction of colonies and their size at λ~80 nm leads to a significant increase in δ and σ_B. Achieving high strength and plasticity was ensured by an increase in the volume fraction of particles of the γ- and β-phases.